Journal of Biological Methods | **2015** | Vol. 2(3) | e28 DOI: 10.14440/jbm.2015.77

Deciphering hepatocellular responses to metabolic and oncogenic stress

Marcelo et al.

Supplementary Information

Figure S1. Percent yield of $CD45^+$ liver NPF fraction after MACS and gating strategy for isolation of $F4/80^+$ and VE-cad^+ cells.
Figure S2. Assessment of cell surface marker expression within $CD95^+$ fractions of the liver PF via FACS and fluorescence immunohistochemistry.
Figure S3. Assessment of cell surface marker expression within $F4/80^+$ fractions of the liver NPF via FACS and fluorescence immunohistochemistry.
Figure S4. Assessment of cell surface marker expression within VE-cad^+ fractions of the liver NPF via FACS and fluorescence immunohistochemistry.
Figure S5. Effect of metabolic and oncogenic stress on cell number and gene expression of various hepatic cell subfractions.
Figure S6. Comparison of gene expression signature from HFD-treated hepatic cell types to a murine obese liver gene set.
Figure S7. Gene ontological analyses observed between HFD-treated liver cell types and human obese gene set.
Figure S8. Gene ontological analyses observed between DEN-treated liver cell types and human HCC gene set.
Table S1. Anti-mouse antibodies and their respective fluorochrome conjugates used for flow cytometric analysis.
Table S2. Primary antibodies used in immunohistochemical staining of liver sections.
Table S3. List of actual magnifications for histological and cell culture images in each figure.

Supplementary information of this article can be found online at http://www.jbmethods.org/jbm/rt/suppFiles/77.

A. CD45+ Enrichment After MACS

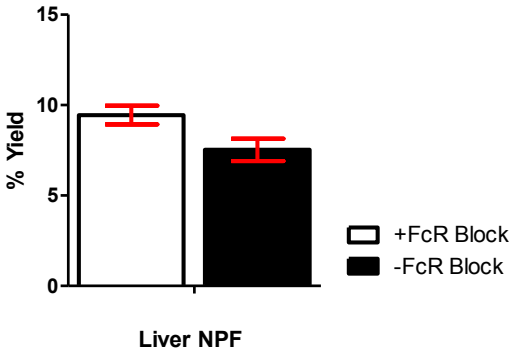

B.

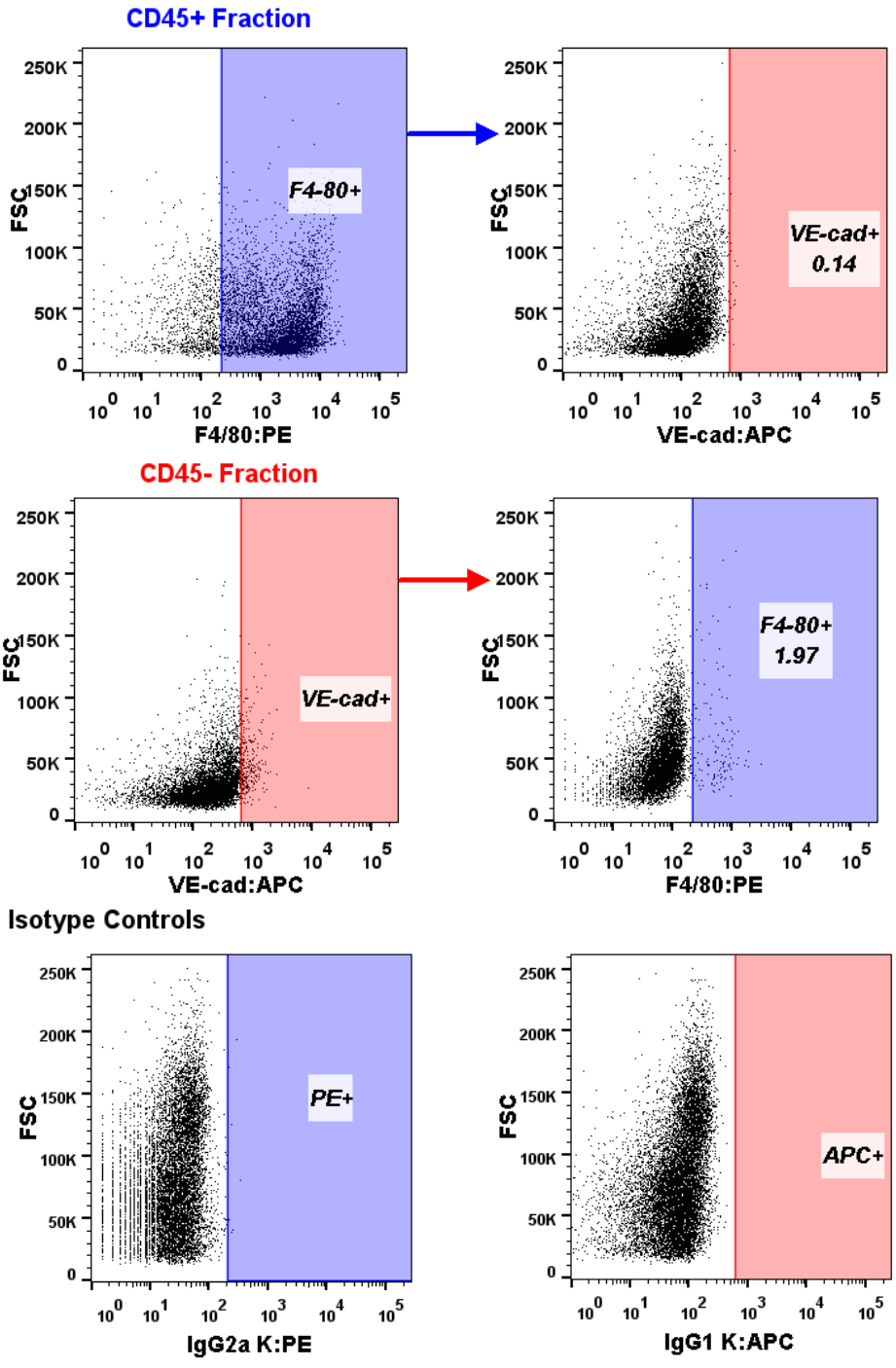

Figure S1. A. Comparison of percent yield of $CD45^+$ fraction isolated from liver NPF following enrichment via MACS, with or without an FcR block step. **B.** Gating strategy for isolation of $F4/80^+$ cells within $CD45^+$ fraction (blue gate, top panels), and of $VE\text{-}cad^+$ cells within $CD45^-$ fraction (red gate, bottom panels) from liver. Also shown are representative plots for assessment of contaminating $VE\text{-}cad^+$ cells (red gate, top panels) within $F4/80^+CD45^+$ macrophage fraction (blue gate, top), and contaminating $F4/80^+$ cells (blue gate, bottom panels) within $VE\text{-}cad^+CD45^-$ SEC fraction (red gate, bottom panels). The percentage values of contaminating cells, as indicated within each gate, are negligible. FACS plots showing staining using IgG isotype control are also shown.

***

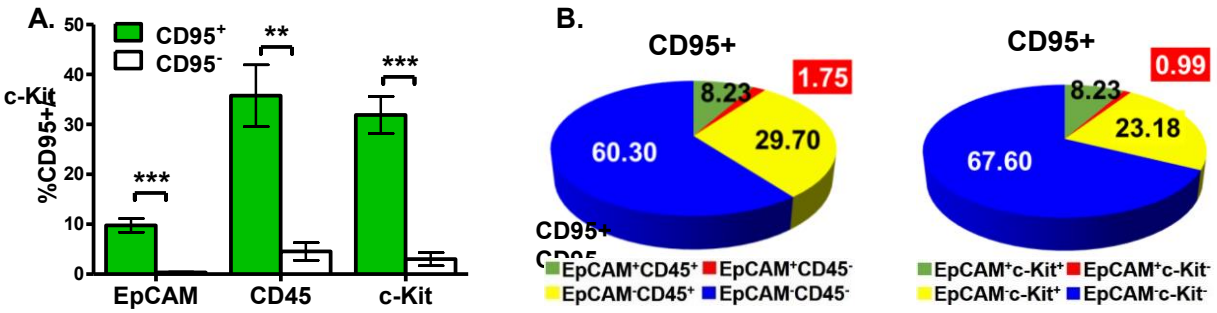

C. CD95 Alb DAPI Merge

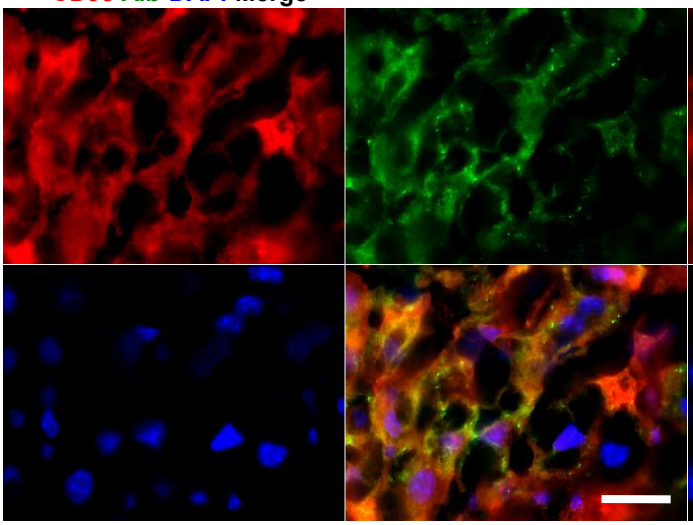

D. CD95 CK8 DAPI Merge

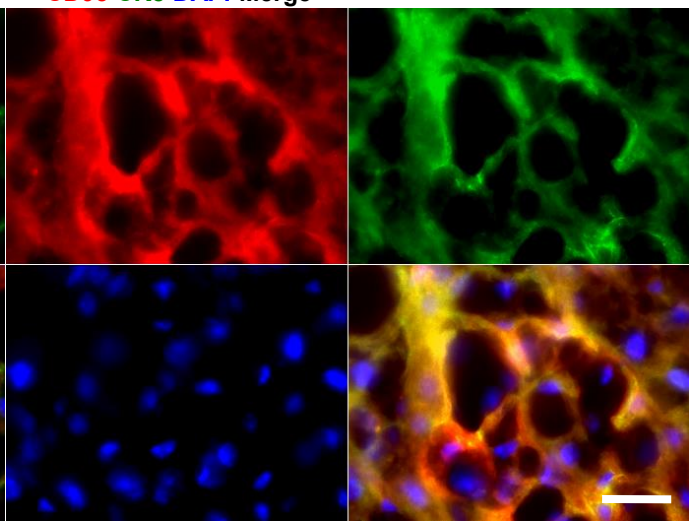

E. CD95 EpCAM DAPI Merge

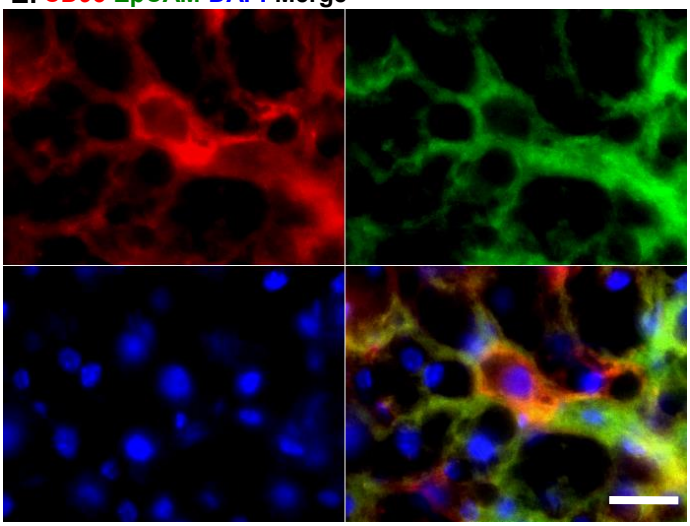

Figure S2. A. Frequency of antigenic cell surface marker expression by $CD95^+$ versus $CD95^-$ cells of the liver parenchymal fraction, as determined by flow cytometry. **B.** Proportion of $CD95^+$ PH co-expressing select cell surface markers commonly associated with hepatocytes. **C-E.** Fluorescence immunostaining of normal murine liver reveals co-expression of CD95 (red) with the mature hepatocyte markers Albumin (Alb, **C**), cytokeratin 8 (CK8, **D**) and Epithelial Cell Adhesion Molecule (EpCAM, **E**). All scale bars represent 20 μm.

A.

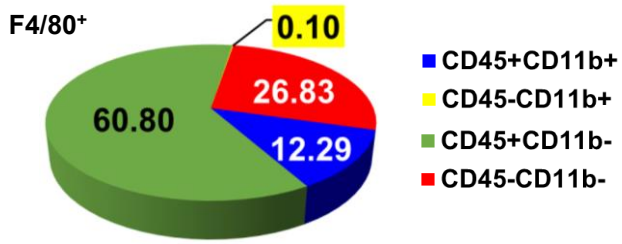
F4/80+
0.10
26.83
60.80
12.29
CD45+CD11b+
CD45-CD11b+
CD45+CD11b-
CD45-CD11b-

B.

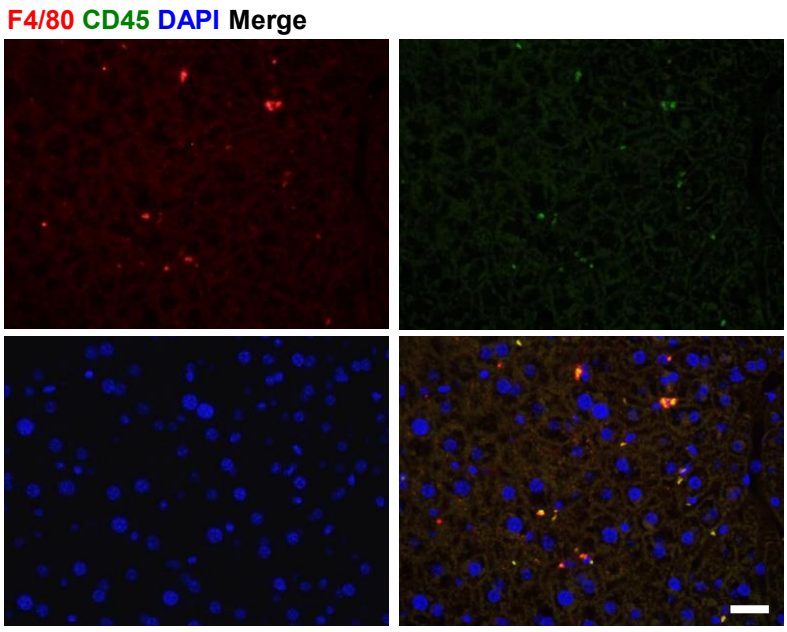
F4/80 CD45 DAPI Merge

C.

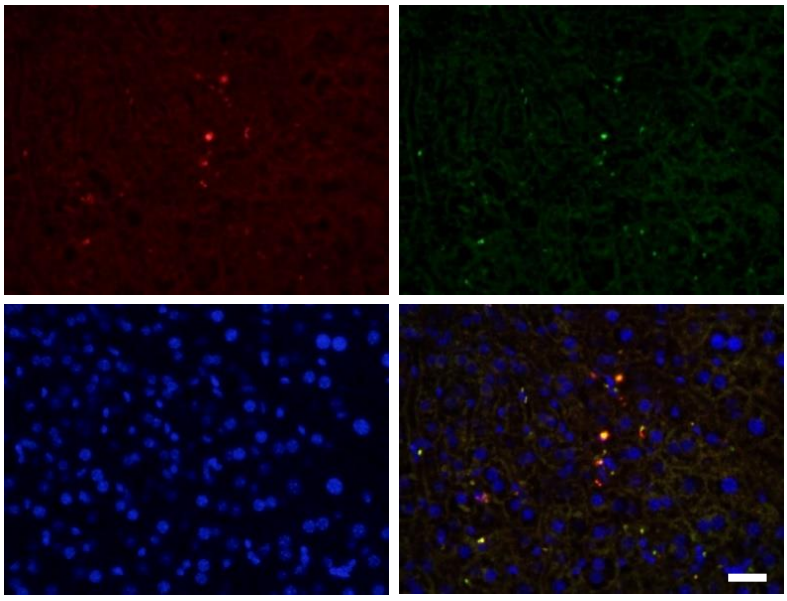
F4/80 CD11b DAPI Merge

Figure S3. A. Distribution of characteristic MΦ surface marker expression on F4/80^{+} cells isolated from liver NPF. **B and C.** Immunostaining of murine liver sections demonstrating co-expression of F4/80 with CD45 (**B**) and F4/80 with CD11b (**C**).

A. CD45$^-$

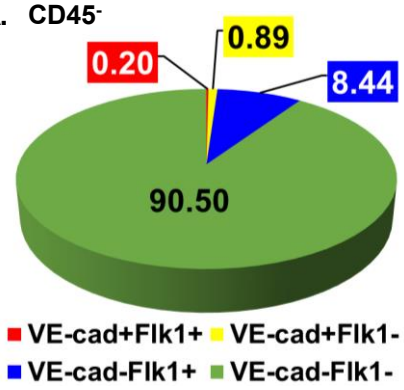

VE-cad$^+$

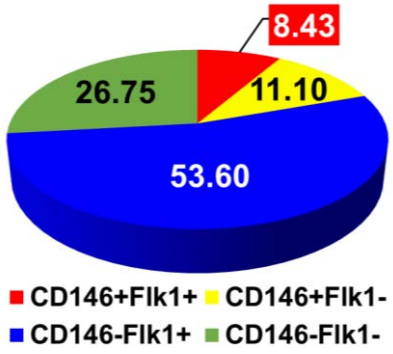

B. VE-cad CD31 DAPI Merge

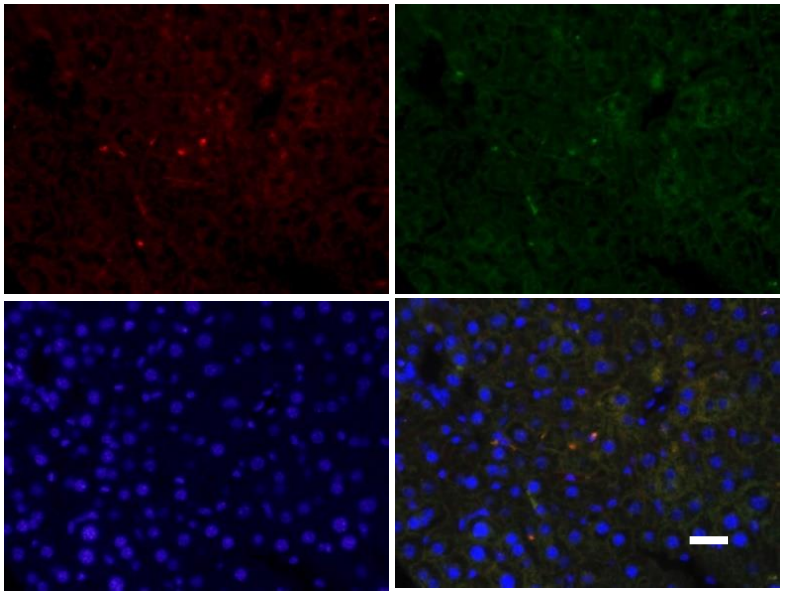

C. VE-cad Flk1 DAPI Merge

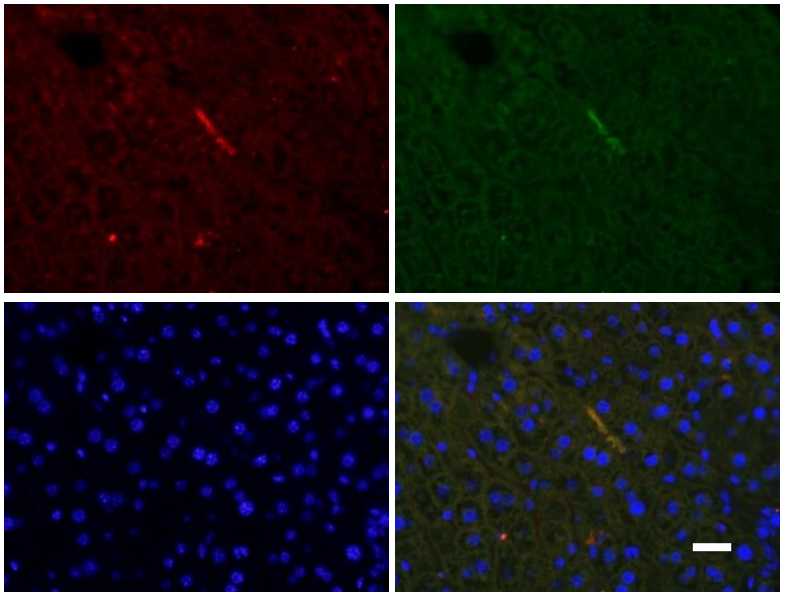

Figure S4. A. Distribution of characteristic SEC surface marker expression on $CD45^-$ or VE-$cadherin^+$ cells isolated from liver NPF. **B and C.** Immunostaining of murine liver sections demonstrating co-expression of VE-cadherin with CD31 (**B**) and Flk1 (**C**) on cells lining the sinusoids. All scale bars represent 20 mm.

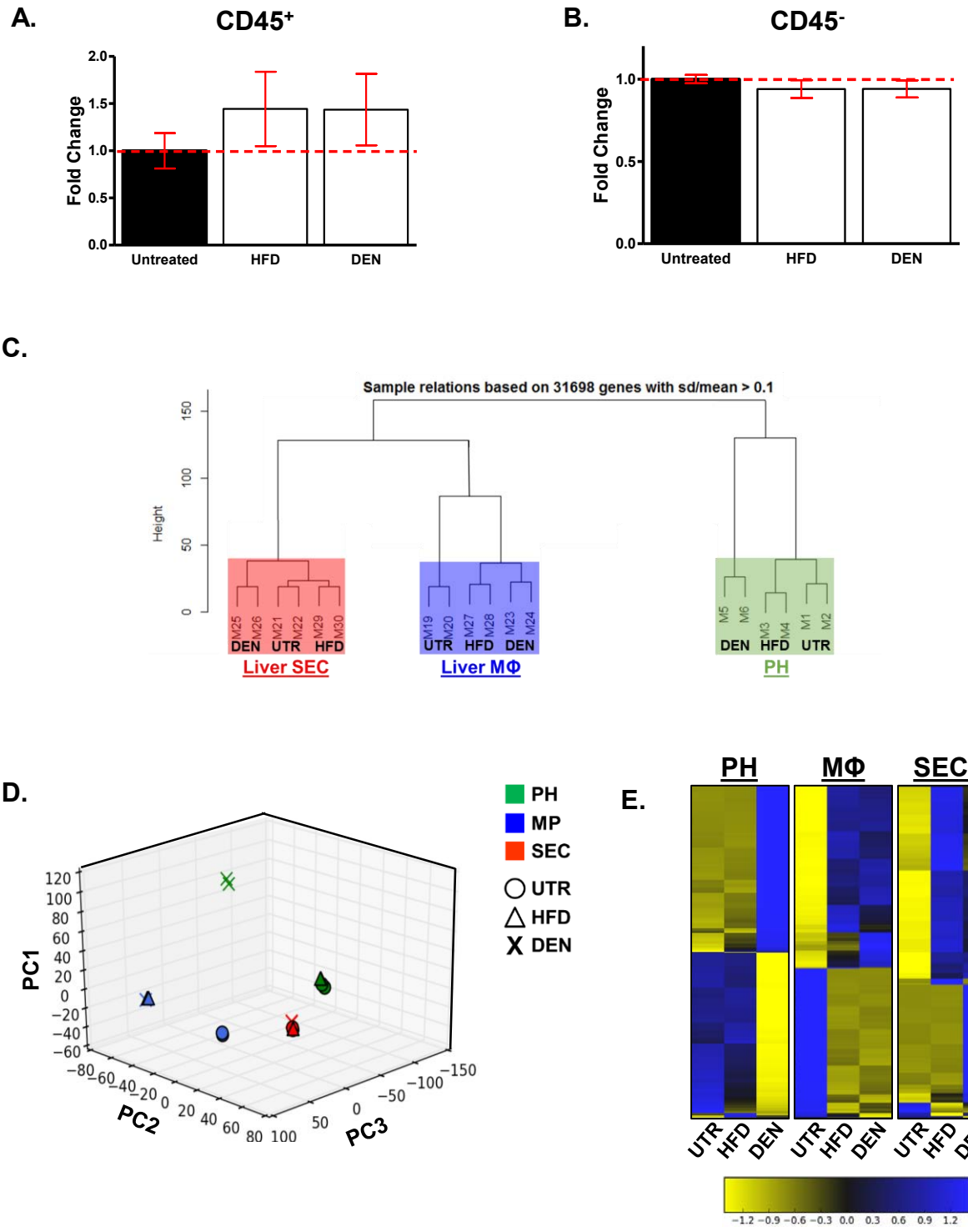
A.
CD45+
Fold Change
2.0
1.5
1.0
0.5
0.0
Untreated
HFD
DEN
B.
CD45-
Fold Change
1.0
0.5
0.0
Untreated
HFD
DEN
C.
Sample relations based on 31698 genes with sd/mean > 0.1
Height
150
100
50
0
M25 M26 M21 M22 M29 M30
DEN UTR HFD
Liver SEC
M19 M20 M27 M28 M23 M24
UTR HFD DEN
Liver MΦ
M5 M6 M3 M4 M1 M2
DEN HFD UTR
PH
D.
PH
MP
SEC
UTR
HFD
DEN
PC1
PC2
PC3
E.
PH
MΦ
SEC
UTR HFD DEN
UTR HFD DEN
UTR HFD DEN
−1.2 −0.9 −0.6 −0.3 0.0 0.3 0.6 0.9 1.2

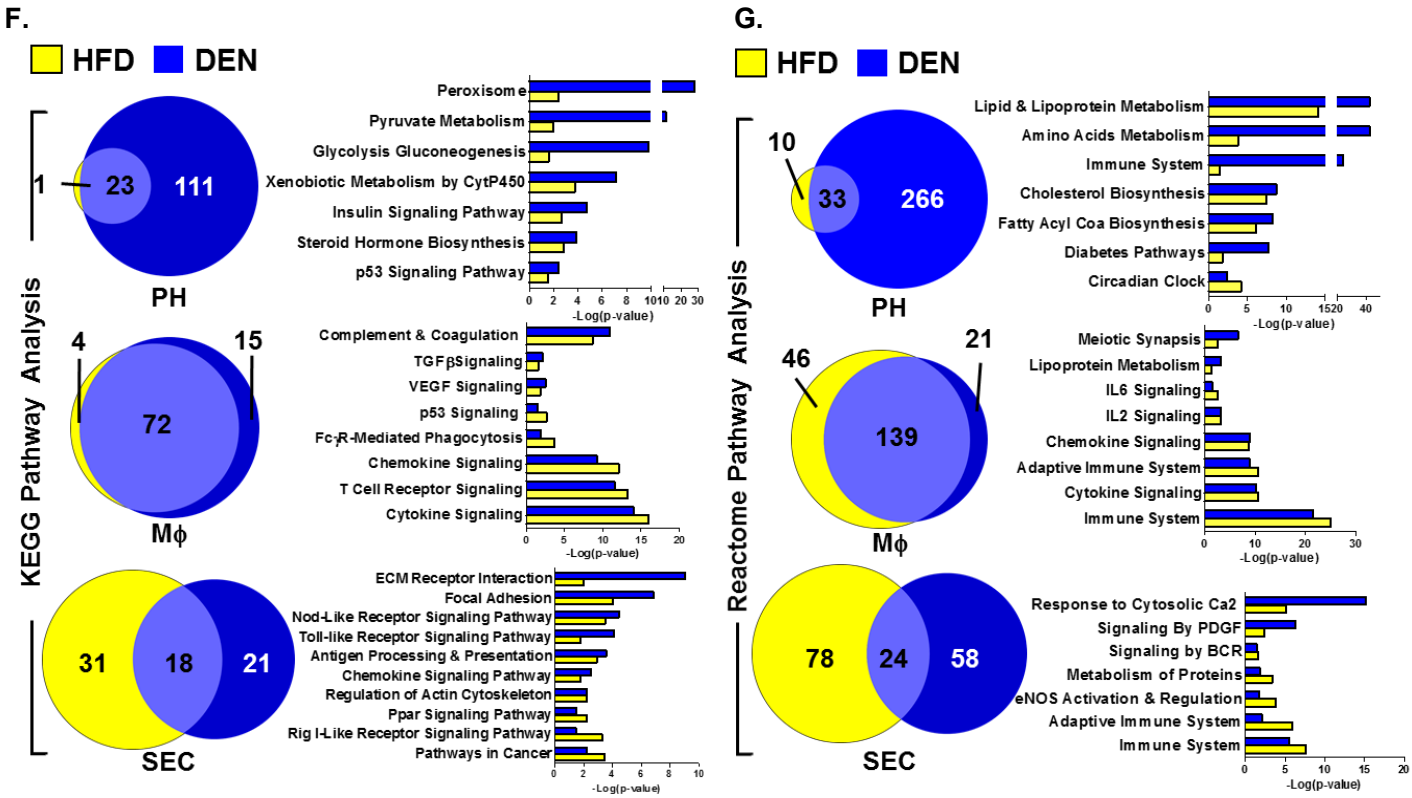
F.
HFD
DEN
KEGG Pathway Analysis
1
23
111
PH
Peroxisome
Pyruvate Metabolism
Glycolysis Gluconeogenesis
Xenobiotic Metabolism by CytP450
Insulin Signaling Pathway
Steroid Hormone Biosynthesis
p53 Signaling Pathway
0 2 4 6 8 10 10 20 30
-Log(p-value)
4
72
15
Mϕ
Complement & Coagulation
TGFβSignaling
VEGF Signaling
p53 Signaling
FcγR-Mediated Phagocytosis
Chemokine Signaling
T Cell Receptor Signaling
Cytokine Signaling
0 5 10 15 20
-Log(p-value)
31
18
21
SEC
ECM Receptor Interaction
Focal Adhesion
Nod-Like Receptor Signaling Pathway
Toll-like Receptor Signaling Pathway
Antigen Processing & Presentation
Chemokine Signaling Pathway
Regulation of Actin Cytoskeleton
Ppar Signaling Pathway
Rig I-Like Receptor Signaling Pathway
Pathways in Cancer
0 2 4 6 8 10
-Log(p-value)
G.
HFD
DEN
Reactome Pathway Analysis
10
33
266
PH
Lipid & Lipoprotein Metabolism
Amino Acids Metabolism
Immune System
Cholesterol Biosynthesis
Fatty Acyl Coa Biosynthesis
Diabetes Pathways
Circadian Clock
0 5 10 1520 40
-Log(p-value)
46
139
21
Mϕ
Meiotic Synapsis
Lipoprotein Metabolism
IL6 Signaling
IL2 Signaling
Chemokine Signaling
Adaptive Immune System
Cytokine Signaling
Immune System
0 10 20 30
-Log(p-value)
78
24
58
SEC
Response to Cytosolic Ca2
Signaling By PDGF
Signaling by BCR
Metabolism of Proteins
eNOS Activation & Regulation
Adaptive Immune System
Immune System
0 5 10 15 20
-Log(p-value)

Figure S5. A and B. Percentages of $CD45^+$ **(A)** and $CD45^-$ **(B)** cells from liver NPF remain unchanged relative to untreated after HFD or DEN treatment. **C.** Hierarchical clustering of normalized microarray data from replicates of PH, MΦ, and SEC isolated from untreated (UTR), HFD, and DEN-treated liver. **D.** Three-dimensional Principal Component Analysis (PCA) plots of replicates of PH, MΦ, and SEC isolated from liver UTR, HFD-, and DEN-treated mice utilized for microarray. **E.** Comparative global gene expression patterns of PH, MΦ, and SEC co-isolated from the liver of UTR, HFD, and DEN-treated mice. **F and G.** Commonality of altered pathways determined via KEGG Pathways **(F)** and Reactome Pathways **(G)** functional analyses observed between PH, MΦ, and SEC isolated from HFD- and DEN-treated murine liver.

A.

	PH	MP	SEC
HFD induced genes (UP)	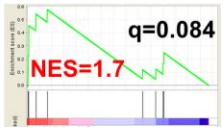	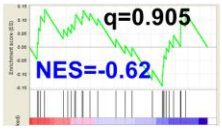	
HFD suppressed genes (DOWN)	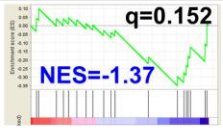	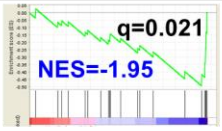	No NES reported

B.

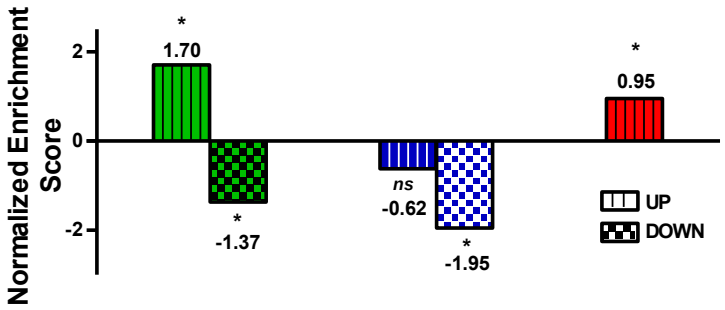

C. [i]

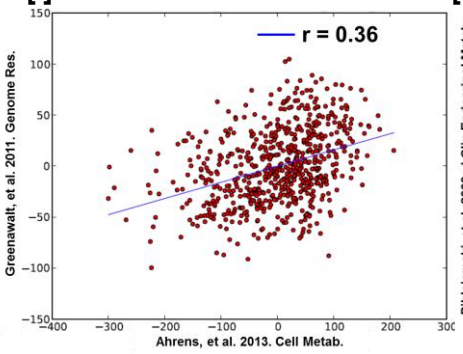

[ii]

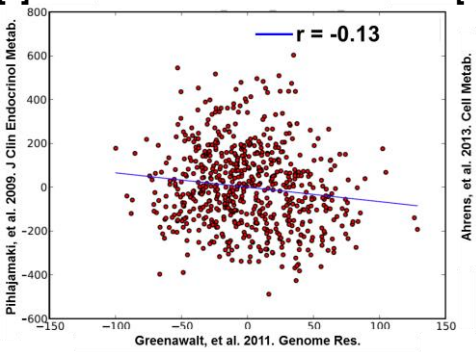

[iii]

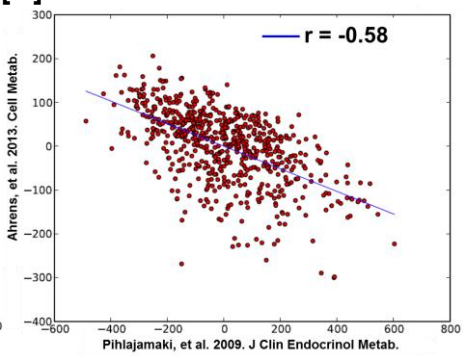

Figure S6. A. Association of gene expression signature of HFD-treated liver PH, MΦ, and SEC with signature derived from murine obese livers [23], via the GSEA method. Of all three cell types, only PH demonstrated a gene expression signature (both upregulated and down-regulated) that matched the murine obese liver signature. **B.** Normalized enrichment scores (NES) of HFD-induced (UP) and HFD-suppressed (DOWN) genes relative to the murine obese liver signature from [23]. **C.** Scatter plots showing correlation of gene expression signature scores between any two of a total of three human obese liver gene data sets [21-22].

Figure S7

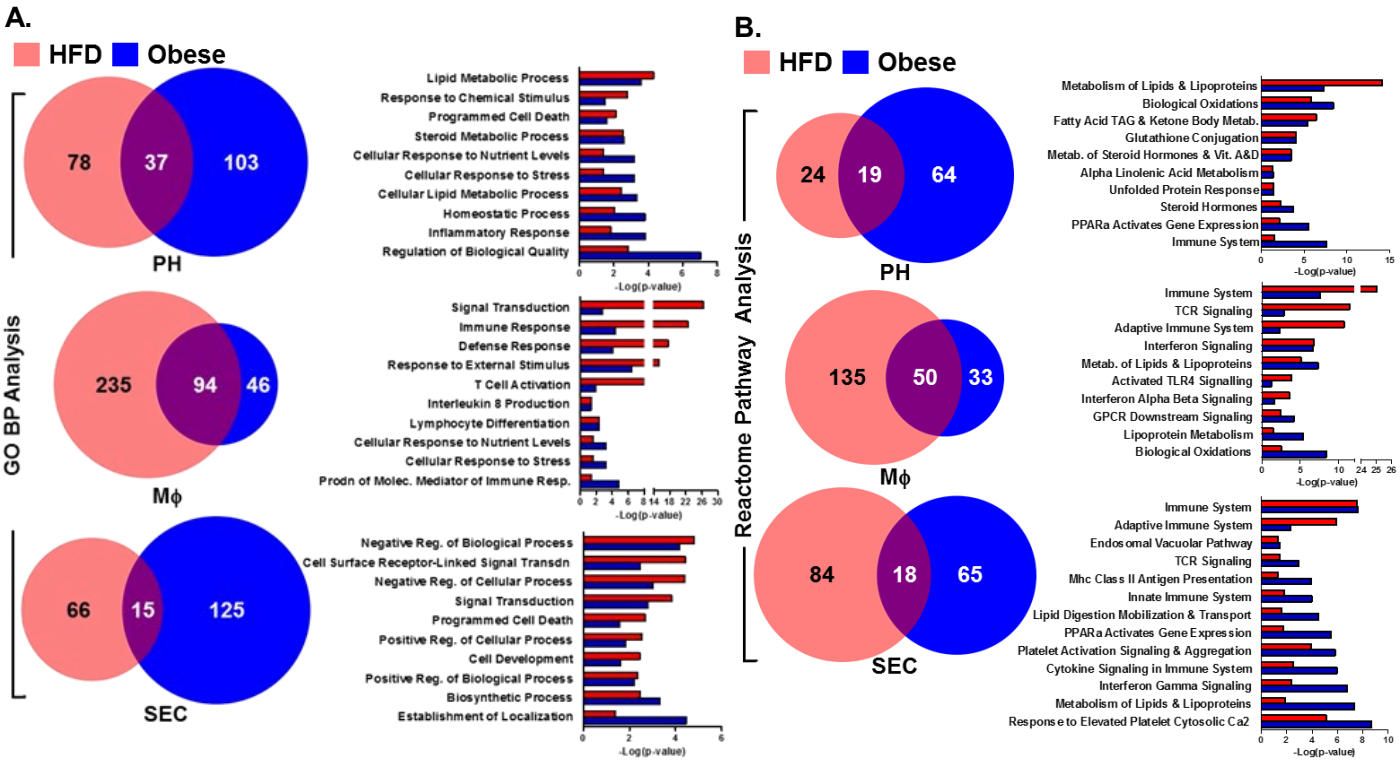
A.
HFD
Obese
78
37
103
PH
235
94
46
Mϕ
66
15
125
SEC
GO BP Analysis
Lipid Metabolic Process
Response to Chemical Stimulus
Programmed Cell Death
Steroid Metabolic Process
Cellular Response to Nutrient Levels
Cellular Response to Stress
Cellular Lipid Metabolic Process
Homeostatic Process
Inflammatory Response
Regulation of Biological Quality
-Log(p-value)
Signal Transduction
Immune Response
Defense Response
Response to External Stimulus
T Cell Activation
Interleukin 8 Production
Lymphocyte Differentiation
Cellular Response to Nutrient Levels
Cellular Response to Stress
Prodn of Molec. Mediator of Immune Resp.
-Log(p-value)
Negative Reg. of Biological Process
Cell Surface Receptor-Linked Signal Transdn
Negative Reg. of Cellular Process
Signal Transduction
Programmed Cell Death
Positive Reg. of Cellular Process
Cell Development
Positive Reg. of Biological Process
Biosynthetic Process
Establishment of Localization
-Log(p-value)
B.
HFD
Obese
24
19
64
PH
135
50
33
Mϕ
84
18
65
SEC
Reactome Pathway Analysis
Metabolism of Lipids & Lipoproteins
Biological Oxidations
Fatty Acid TAG & Ketone Body Metab.
Glutathione Conjugation
Metab. of Steroid Hormones & Vit. A&D
Alpha Linolenic Acid Metabolism
Unfolded Protein Response
Steroid Hormones
PPARa Activates Gene Expression
Immune System
-Log(p-value)
Immune System
TCR Signaling
Adaptive Immune System
Interferon Signaling
Metab. of Lipids & Lipoproteins
Activated TLR4 Signalling
Interferon Alpha Beta Signaling
GPCR Downstream Signaling
Lipoprotein Metabolism
Biological Oxidations
-Log(p-value)
Immune System
Adaptive Immune System
Endosomal Vacuolar Pathway
TCR Signaling
Mhc Class II Antigen Presentation
Innate Immune System
Lipid Digestion Mobilization & Transport
PPARa Activates Gene Expression
Platelet Activation Signaling & Aggregation
Cytokine Signaling in Immune System
Interferon Gamma Signaling
Metabolism of Lipids & Lipoproteins
Response to Elevated Platelet Cytosolic Ca2
-Log(p-value)

Figure S7. Commonality of altered pathways determined via Gene Ontology-Biological Pathways (GO BP) **(A)** and Reactome Pathways **(B)** functional analyses observed between HFD-treated PH, MΦ, or SEC and human obese liver gene signature from [20].

Figure S8

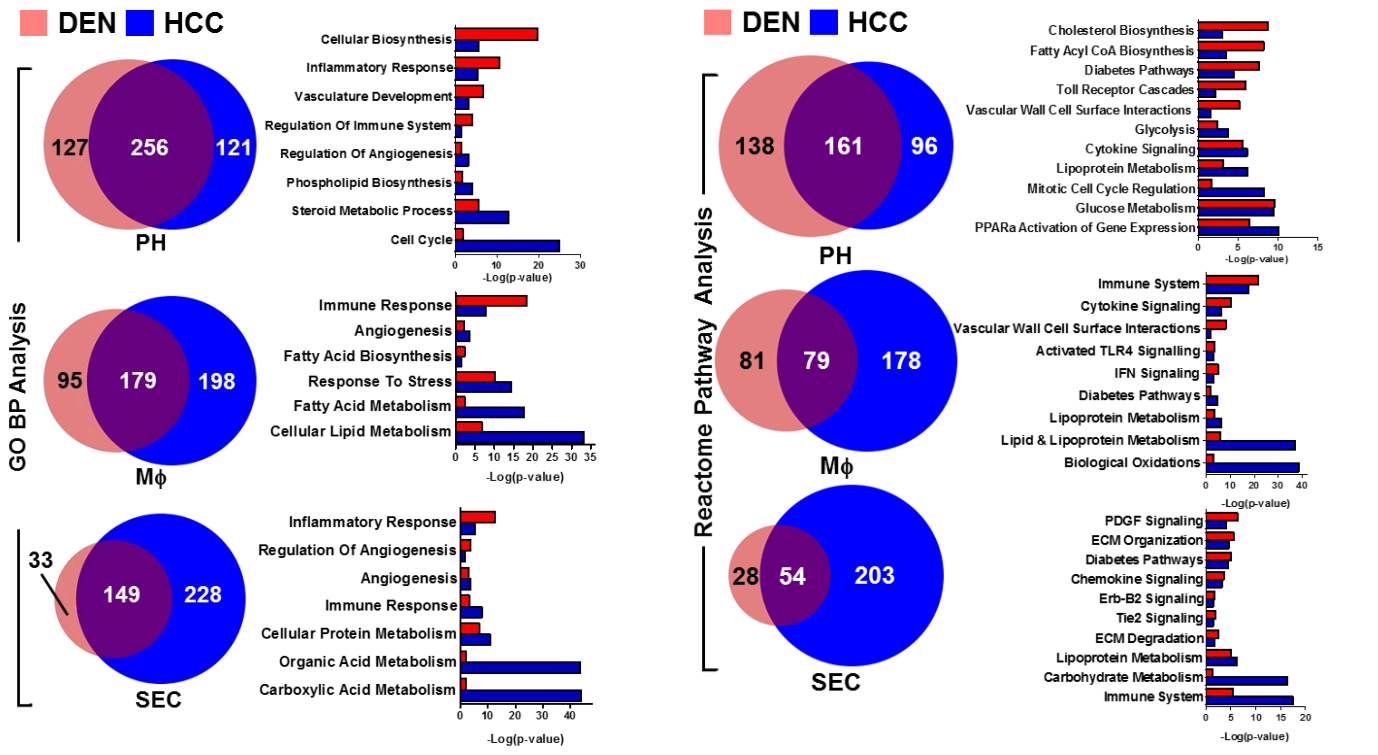
A.
DEN
HCC
127
256
121
PH
Cellular Biosynthesis
Inflammatory Response
Vasculature Development
Regulation Of Immune System
Regulation Of Angiogenesis
Phospholipid Biosynthesis
Steroid Metabolic Process
Cell Cycle
-Log(p-value)
GO BP Analysis
95
179
198
Mϕ
Immune Response
Angiogenesis
Fatty Acid Biosynthesis
Response To Stress
Fatty Acid Metabolism
Cellular Lipid Metabolism
-Log(p-value)
33
149
228
SEC
Inflammatory Response
Regulation Of Angiogenesis
Angiogenesis
Immune Response
Cellular Protein Metabolism
Organic Acid Metabolism
Carboxylic Acid Metabolism
-Log(p-value)
B.
DEN
HCC
Reactome Pathway Analysis
138
161
96
PH
Cholesterol Biosynthesis
Fatty Acyl CoA Biosynthesis
Diabetes Pathways
Toll Receptor Cascades
Vascular Wall Cell Surface Interactions
Glycolysis
Cytokine Signaling
Lipoprotein Metabolism
Mitotic Cell Cycle Regulation
Glucose Metabolism
PPARa Activation of Gene Expression
-Log(p-value)
81
79
178
Mϕ
Immune System
Cytokine Signaling
Vascular Wall Cell Surface Interactions
Activated TLR4 Signalling
IFN Signaling
Diabetes Pathways
Lipoprotein Metabolism
Lipid & Lipoprotein Metabolism
Biological Oxidations
-Log(p-value)
28
54
203
SEC
PDGF Signaling
ECM Organization
Diabetes Pathways
Chemokine Signaling
Erb-B2 Signaling
Tie2 Signaling
ECM Degradation
Lipoprotein Metabolism
Carbohydrate Metabolism
Immune System
-Log(p-value)

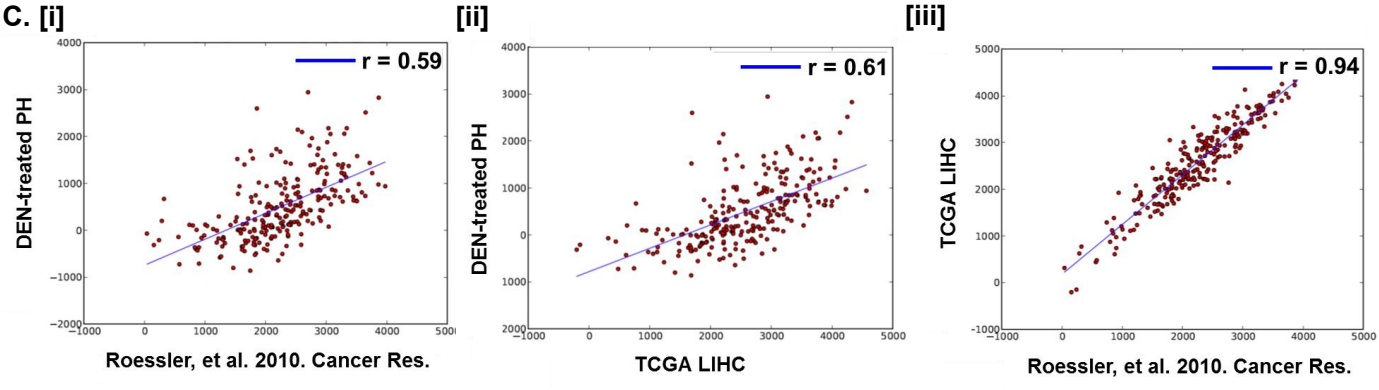
C. [i]
r = 0.59
DEN-treated PH
Roessler, et al. 2010. Cancer Res.
[ii]
r = 0.61
DEN-treated PH
TCGA LIHC
[iii]
r = 0.94
TCGA LIHC
Roessler, et al. 2010. Cancer Res.

Figure S8. A and B. Commonality of altered pathways determined via Gene Ontology-Biological Pathways (GO BP) **(A)** and Reactome Pathways **(B)** functional analyses observed between DEN-treated PH, MΦ, or SEC and human HCC gene signature from [18,19]. **C.** Scatter plots showing correlation of gene expression signatures between **[i]** DEN-treated PH and human HCC gene set from [18,19]. **[ii]** DEN-treated PH and human HCC gene set from TCGA-LIHC, and **[iii]** human HCC gene sets from [18,19] and TCGA-LIHC.

SUPPLEMENTARY TABLES

Supplementary Table 1. Anti-mouse antibodies and their respective fluorochrome conjugates used for flow cytometric analysis.

Antigen/Target	**Fluorochrome Conjugate**	**Clone**
Hepatocyte Markers		
CD95	APC	15A7
Epithelial Cell Adhesion Molecule (EpCAM)	PE-Cy7	G8.8
c-Kit	PE	2B8
CD45	eFluor 780	30-F11
Macrophage Markers		
F4/80	PE	BM8
CD45	eFluor 780	30-F11
CD11b	PE-Cy7	M1/70
CD16/32	AlexaFluor 700	93
Endothelial Cell Markers		
VE-cadherin	APC, eFluor 450	BV13
CD31	APC	390
Flk1	PE	Avas12α1
CD105	PE	Mj7/18
CD146	FITC	P1H12

Supplementary Table 2. Primary antibodies used in immunohistochemical staining of liver sections.

Antigen/Target	**Host Species**	**Clone**
CD95	Mouse	15A7
Albumin	Rat	1D6
EpCAM	Rat	G8.8
Cytokeratin 8 (CK8)	Rat	SP2/0
F4/80	Goat	A-19
CD45	Rat	30-F11
VE-cadherin	Goat	NS0
CD31	Rat	MEC 13.3

Supplementary Table 3. List of actual magnifications for histological and cell culture images in each figure.

Figure	**Scale bar (μm)**	**Image Magnification**
1A[i]	20	228.6
2B[i]	20	228.6
2B[ii]	20	457.2
2B[iii]	20	457.2
2C[i]	20	228.6
2C[ii[	20	228.6
3C[i]	20	317.5
3C[ii]	20	317.5
3C[iii]	20	317.5
3C[iv]	20	317.5
3D[ii]	20	317.5
4C[i]	20	317.5
4C[ii]	20	317.5
4C[iii]	20	317.5
4C[iv]	20	317.5
4E	200	31.75
5C (H&E panels)	20	76.2
5C (IHC panels)	20	152.4